



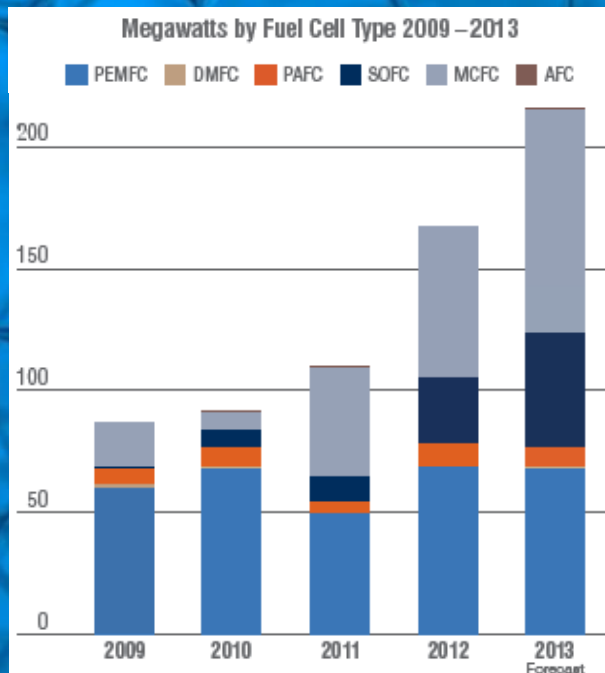
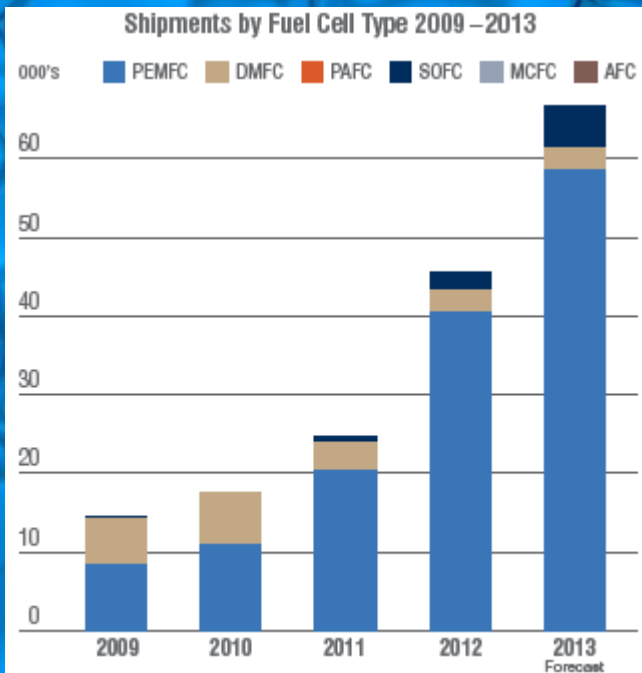
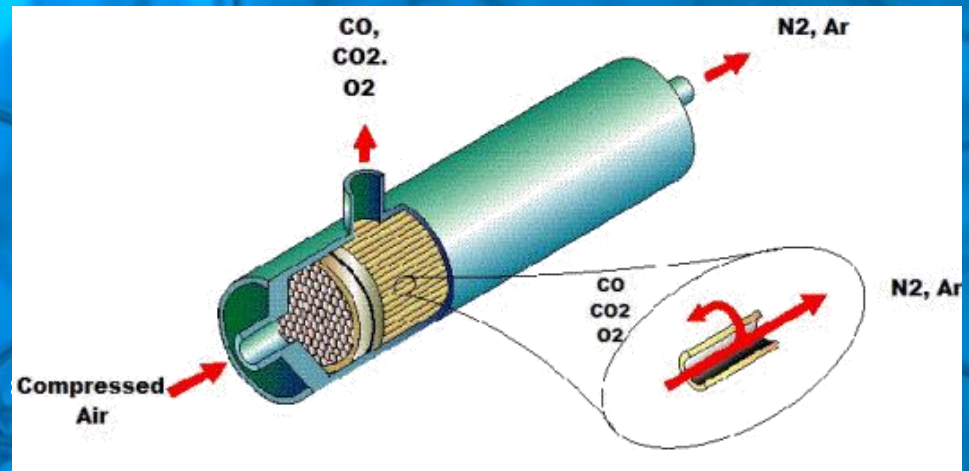
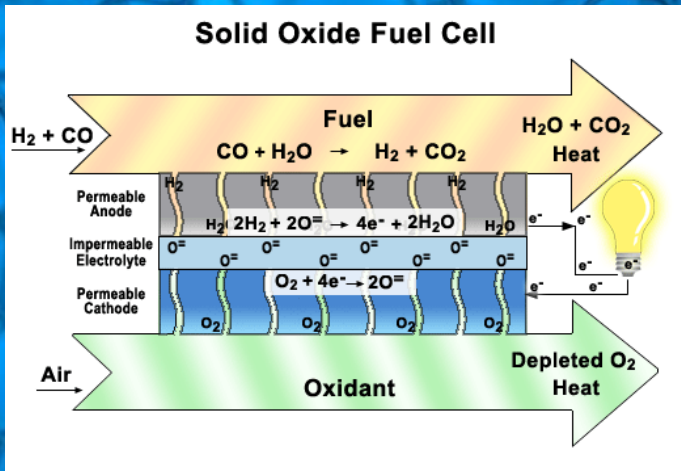
Application of SR methods for the study of nanocomposite materials for Hydrogen Energy.

Speaker: VINOKUROV, ZAKHAR

Co-authors: PAVLOVA, S.N.; EREMEEV, N.F.; SADYKOV, V.A.; KRIVENTSOV, V.V.

Boreskov Institute of Catalysis SB RAS, Novosibirsk, Russia

Materials with mixed ionic–electronic conductivity



Solid oxide fuel cells (SOFC)

Oxygen separation membranes

Hydrocarbon fuel reforming

IT SOFC cathode materials

$\text{PrNi}_{1-x}\text{Co}_x\text{O}_{3-\delta}$ (PNCx, $x= 0-0.6$); $\text{Ce}_{0.9}\text{Y}_{0.1}\text{O}_{2-\delta}$ (YDC); nanocomposites PNCx-YDC

Synthesis of nanocomposites:

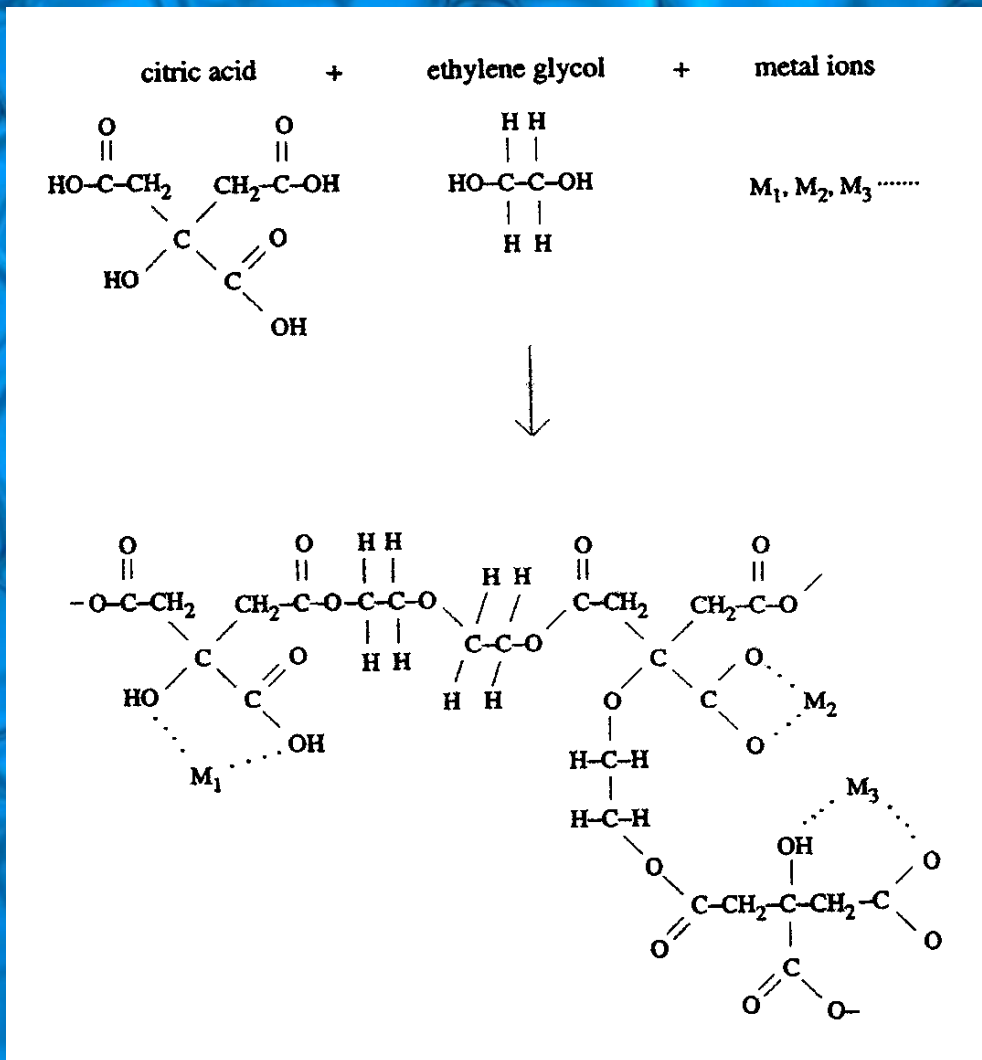
By ultrasonic dispersion of powders mixtures in solvents with addition of surfactants, compacting into pellets/supporting layers and sintering up to 1300°C

Structure and composition: XRD , TEM +EDX

Activity in O_2 dissociation and oxygen mobility:

O_2 TPD, $^{18}\text{O}_2$ and C^{18}O_2 isotope exchange (SSITKA), XRD SR unit cell relaxation (UCR), weight & conductivity relaxation

Basic method of synthesis – modified Pechini route

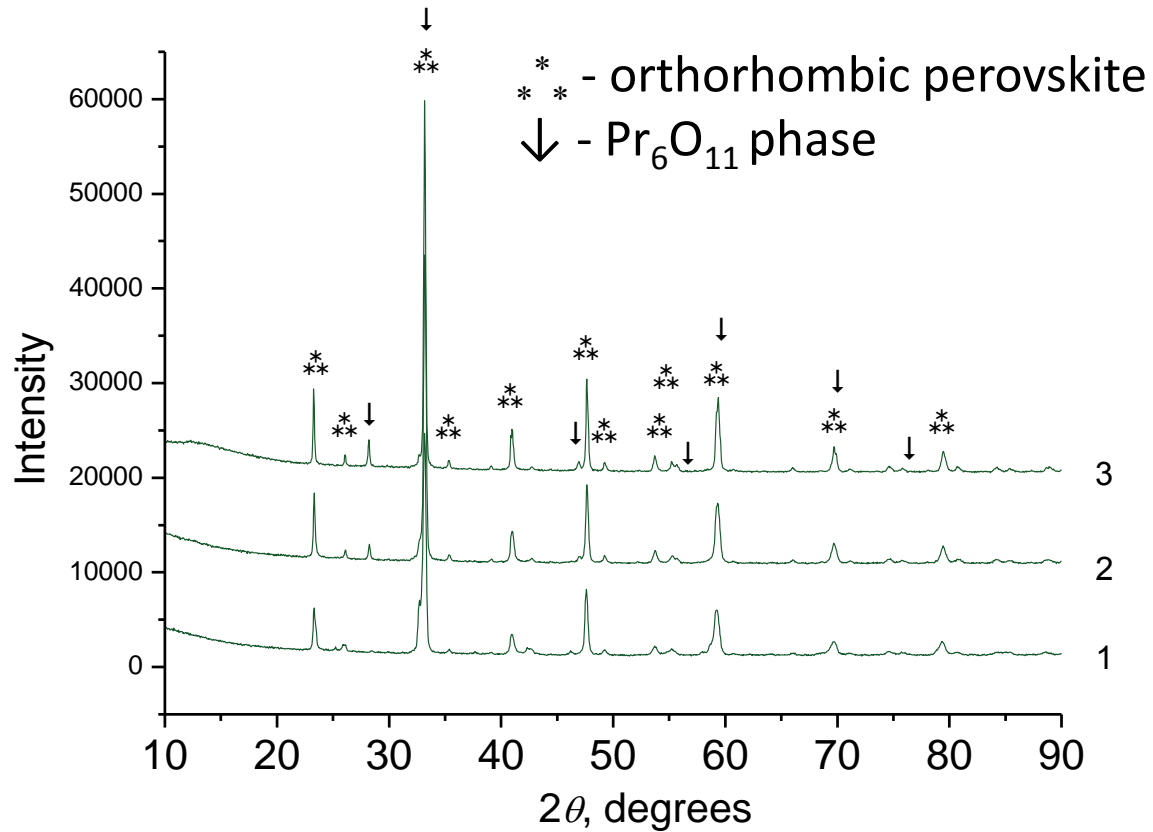


Formation of solid polymeric matrix at heating of solution followed by burning

Fixation of cations, helps to suppress phase segregation and spatial non-uniformity.

Crystalline phases are formed starting from 250-300 C under air calcination.

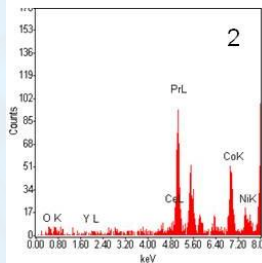
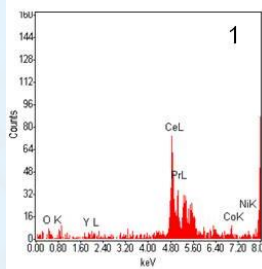
XRD PNCx



Sintered at 1100°C . Co $x = 0.6$ (1), 0.5 (2) and 0.4 (3).
Amount of Pr_6O_{11} admixture increases with Ni content

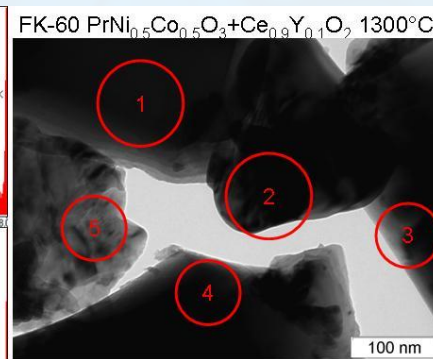
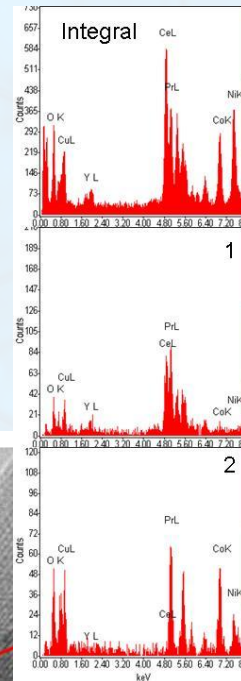
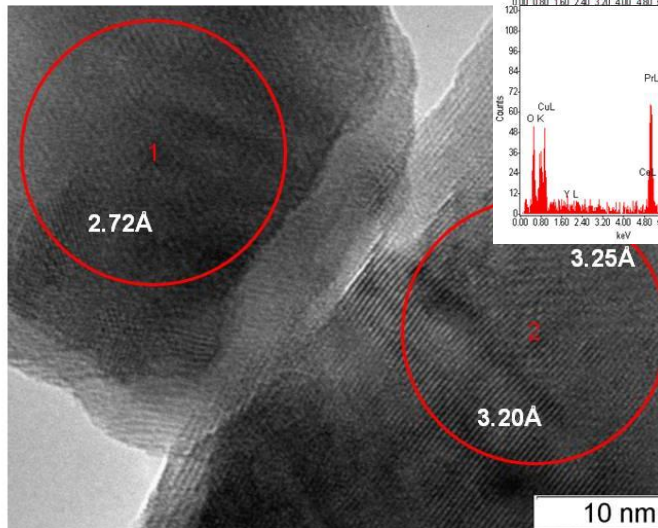
TEM with EDX: PNC-YDC

Domains of doped ceria contains up to 30% of Pr after sintering at 1100°C and up to 50% after sintering at 1300°C.

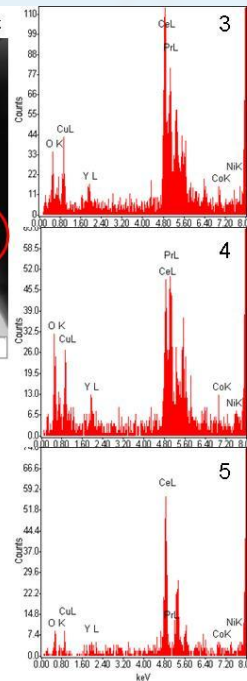


Atomic % by Element

	Y L	Ce L	Pr L	Co K	Ni K
1	1.93	63.43	29.7	3.4	1.54
2	0	0	70.45	22.16	7.39

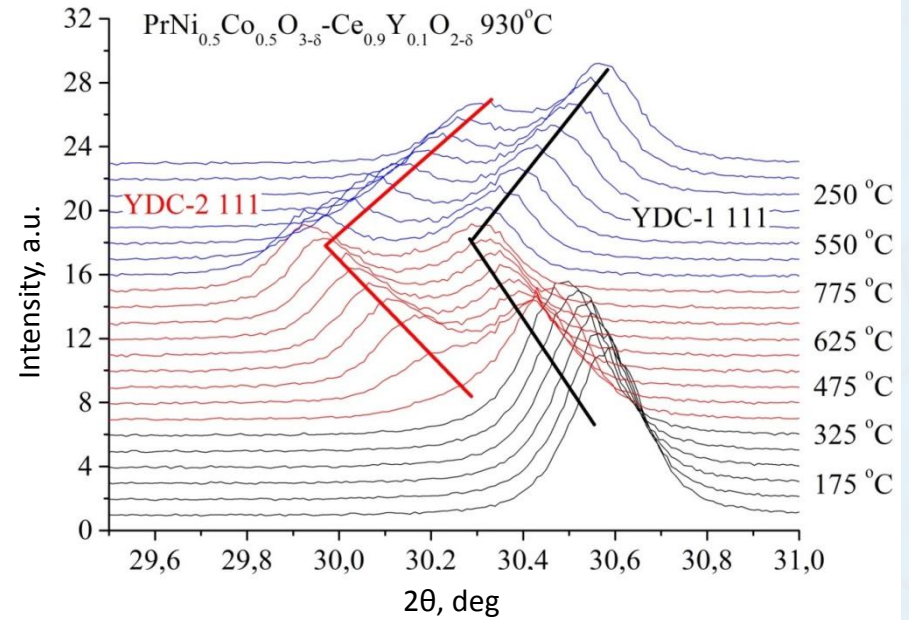
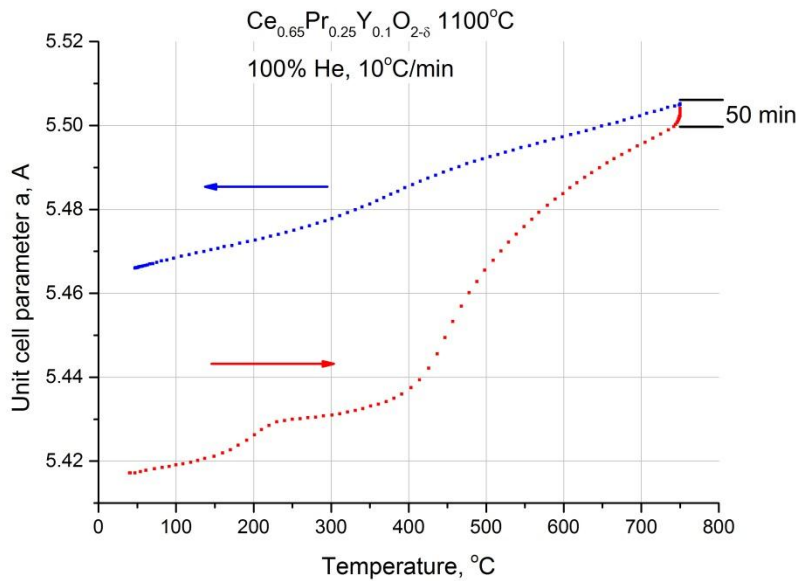


	Y L	Ce L	Pr L	Co K	Ni K
integral	2.8	42.24	27.72	11.32	15.93
1	3.8	41.28	50.63	2.64	1.65
2	0	2.54	63.08	23.56	10.81
3	2.96	54.49	39.23	1.93	1.39
4	5.05	40.87	52.14	0.9	1.05
5	4.17	92.84	0	1.95	1.03



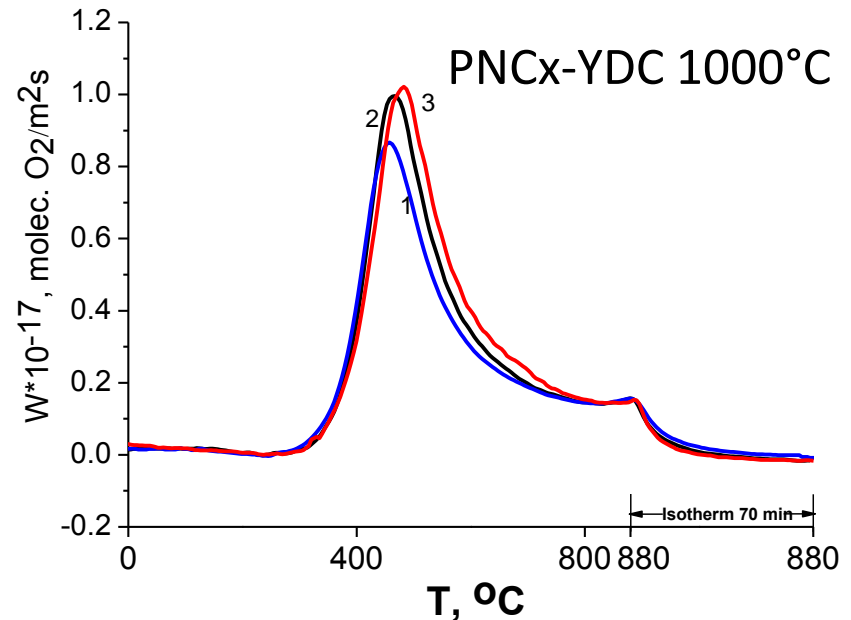
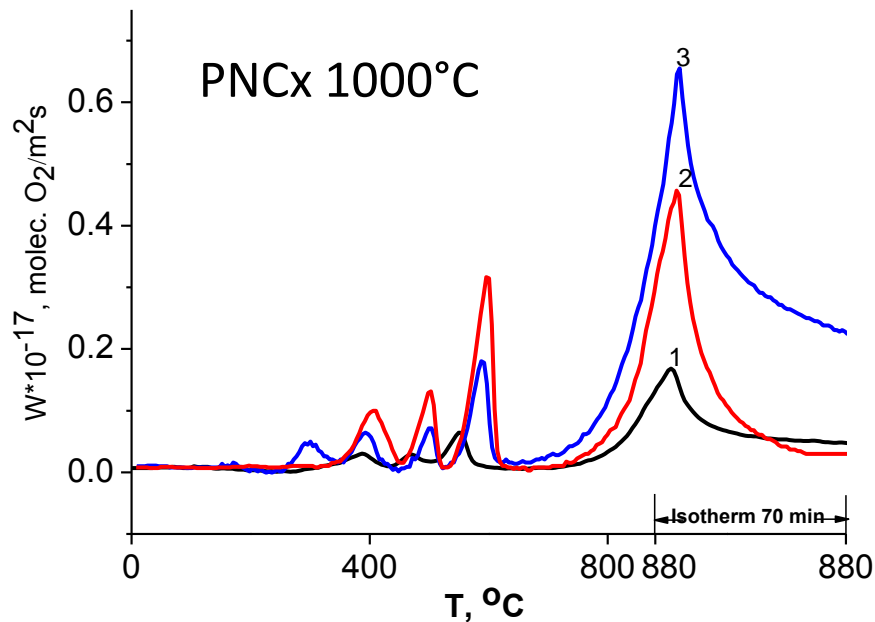
Incorporation of Pr cations into doped ceria phase disorders both perovskite-like and fluorite-like phases.

Redistribution of Pr in PNC0.5-YDC



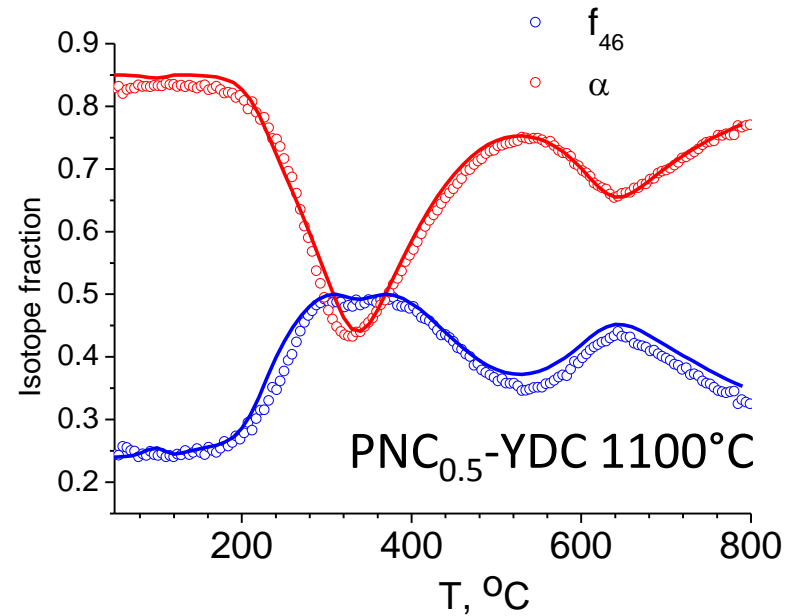
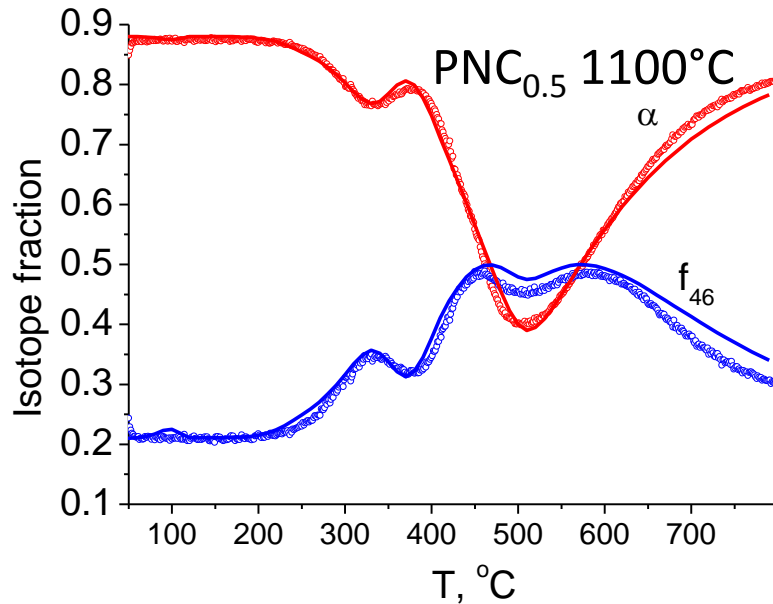
$\text{Ce}_{0.65}\text{Pr}_{0.25}\text{Y}_{0.1}\text{O}_{2-\delta}$ 1100°C(left); PNC0.5-YDC 930°C heating in He(right).
 (111) reflection splitting of fluorite-like phase caused by oxygen loss of
 YDC-2 with incorporated Pr.

O₂ temperature programmed desorption



Co x = 0.6 (1), 0.5 (2) and 0.4 (3). PNCx- several separated narrow peaks, desorption is associated with several states of bulk oxygen (defects, restructuring). Much higher oxygen mobility in nanocomposites, desorption at lower temperatures of up to 50 oxygen monolayers ~1% of total oxygen content \Rightarrow lower barriers for oxygen diffusion in the bulk. Oxygen mobility tends to slightly decrease with Co content

C¹⁸O₂ SSITKA



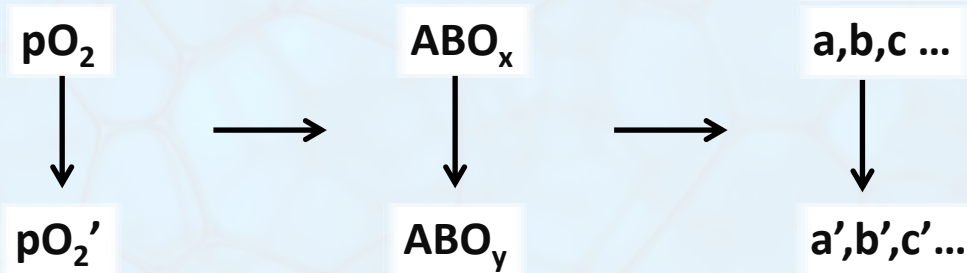
Points – experiment; lines – fitting.

Good fitting by model with two bulk oxygen forms with $D_I/D_{II} \sim 10^3$

Much better sensitivity of C¹⁸O₂ exchange to bulk diffusion due to by 3 order higher rates of exchange as compared with ¹⁸O₂ exchange

Much higher oxygen mobility in nanocomposites due to fast channel domination

XRD UCVR basics

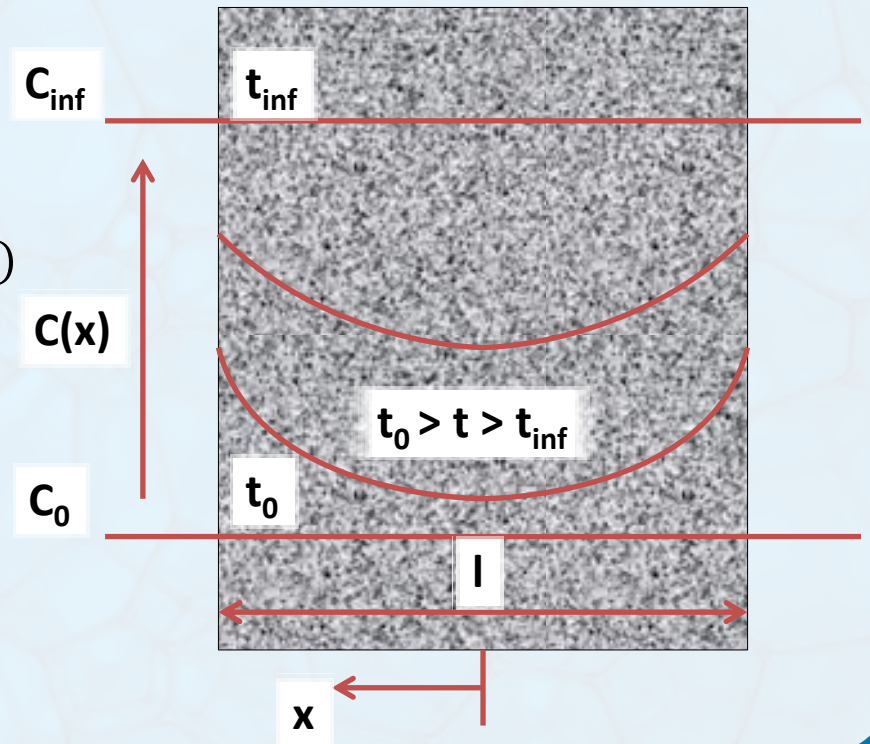


$$\frac{\sigma - \sigma_0}{\sigma_0 - \sigma_\infty} = \frac{m - m_0}{m_0 - m_\infty} =$$

$$1 - \sum_{n=0}^{\infty} \frac{2L^2}{\beta_n^2(\beta_n^2 + L^2 + L)} \exp(-4\beta_n^2 D_{chem} t / l^2)$$

$$L = \frac{lk_{chem}}{2D_{chem}}, \beta_n \tan(\beta_n) = L \quad [1]$$

Can be used for volume cell relaxation if
 $\partial V / \partial t \propto \partial C / \partial t$ и $\Delta \log(pO_2) < 1$

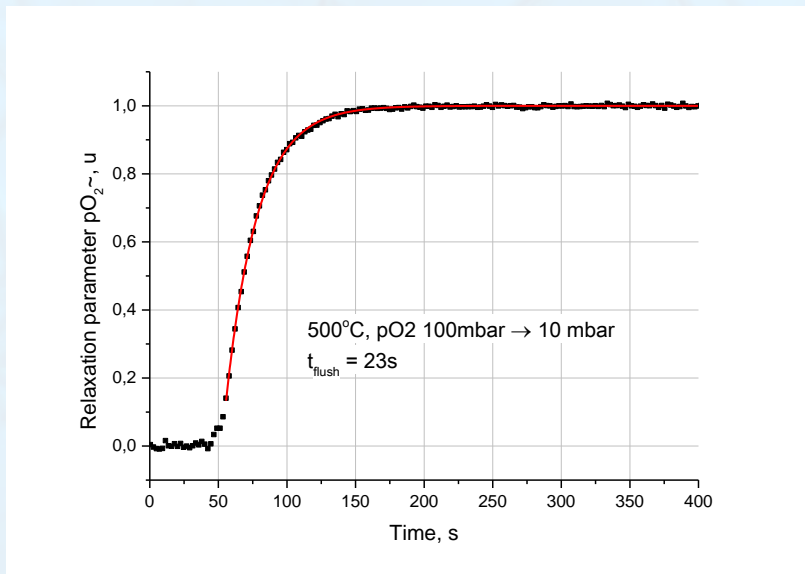


Method restrictions

$$L = \frac{lk_{chem}}{2D_{chem}} \rightarrow l/2 = l_{xrd} \sim 10 \mu\text{m}$$

$L = (0.1 - 10)$ for calculation both k_{chem} and D_{chem}

$\Rightarrow 2 < |\log(k_{chem}) - \log(D_{chem})| < 4$ (optimal 3)



Representative times of the process
 10^2 c (with flush time corrections) $< t < 10^4 \text{ c}$

Impossible to measure if
there are abrupt changes in cell
due to the phase transitions

CPY-1100°C unit cell volume relaxation curves

$$\log(k_{chem}[\text{CM c}^{-1}]) = -5.3 \pm 0.5$$

(XRD SR UCR, 500 °C)

$$\log(k_{chem}[\text{CM c}^{-1}]) = -6.2 \pm 0.1$$

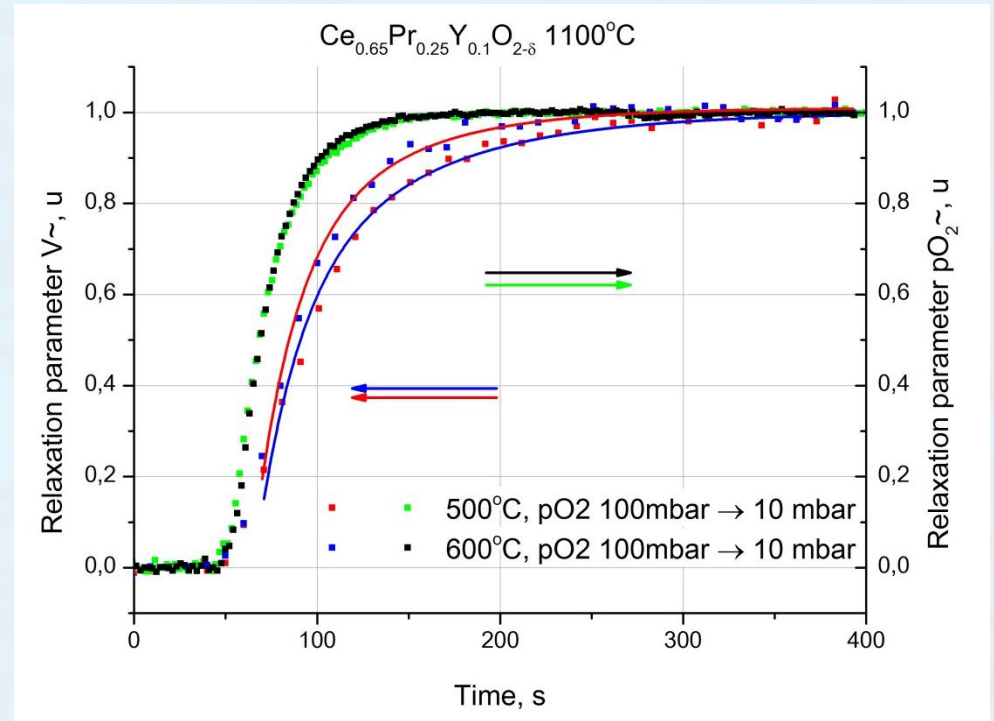
(SSITKA, 500 °C)

$$\log(k_{chem}[\text{CM c}^{-1}]) = -5.2 \pm 0.5$$

(XRD SR UCR, 600 °C)

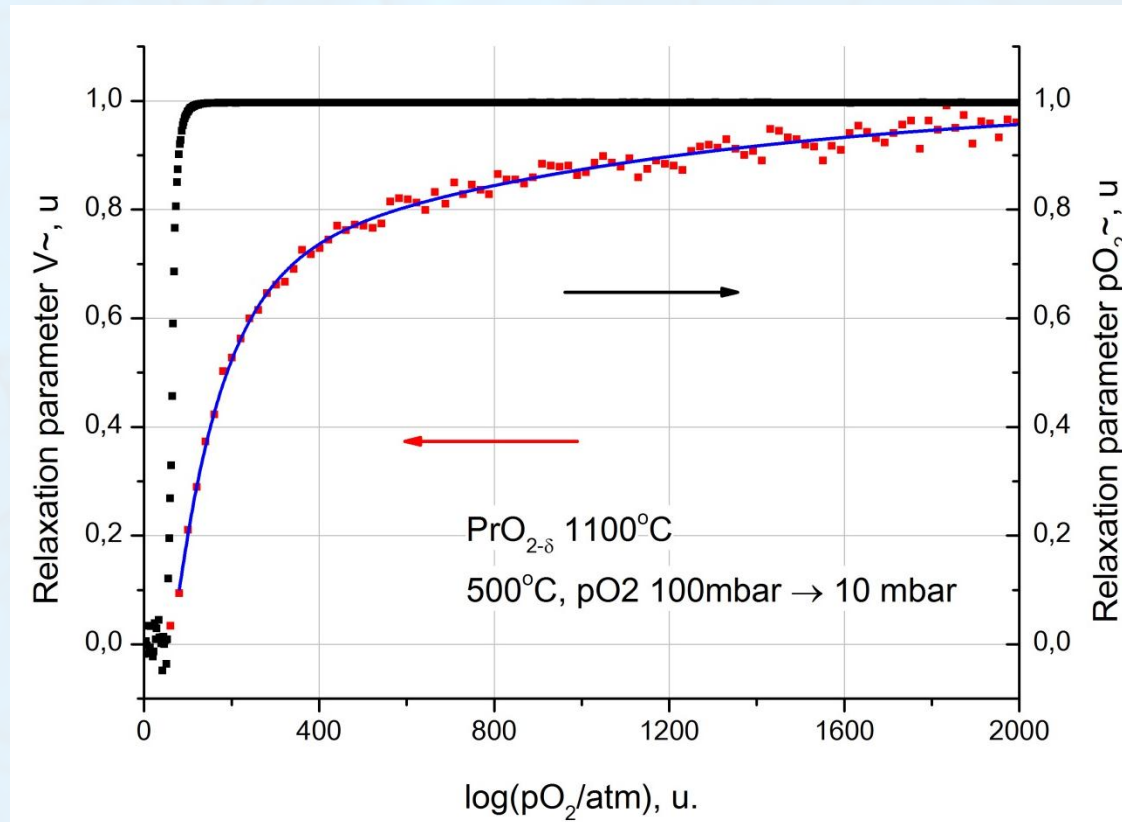
$$\log(k_{chem}[\text{CM c}^{-1}]) = -5.6 \pm 0.1$$

(SSITKA, 600 °C)



XRD SR unit cell relaxation curves for CPY obtained after pO_2 change from 100 to 10 mbar. Points – experiment; lines - fitting.

XRD UCVR PrO_{2-δ}

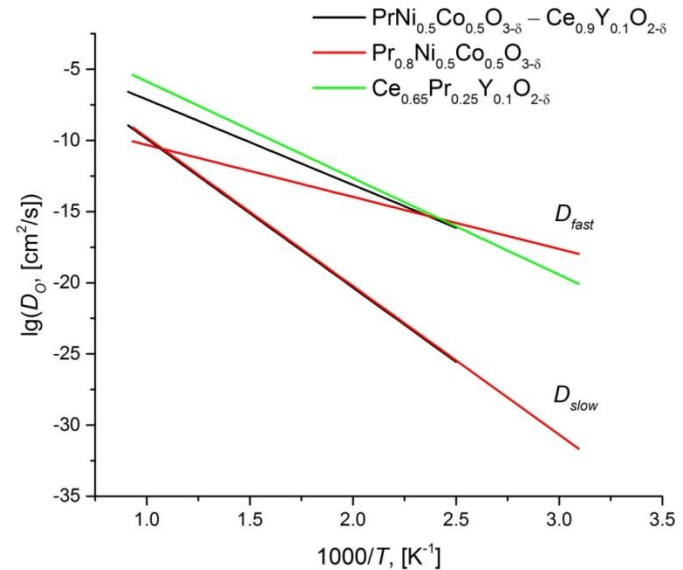
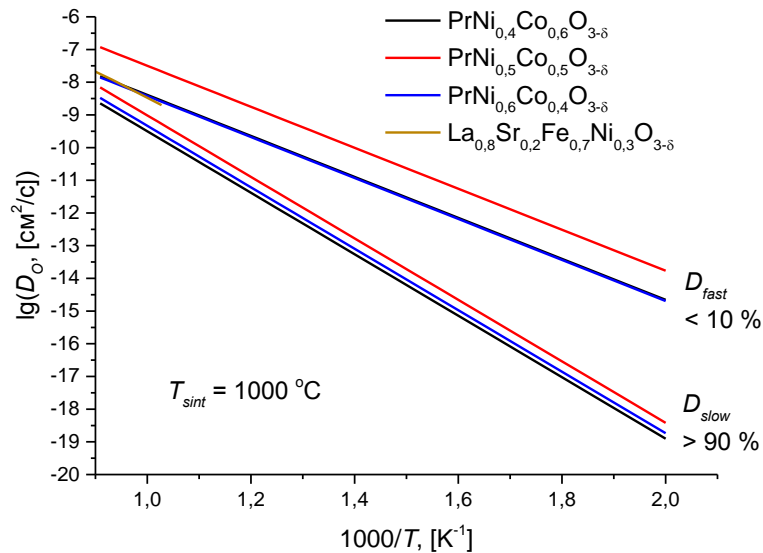


XRD SR unit cell relaxation curves for PrO_{2-δ} obtained after pO₂ change from 100 to 10 mbar. Points – experiment; line - fitting.

$$\log(k_{chem}[\text{CM c}^{-1}]) = -4.5 \pm 0.5 (500 \text{ } ^\circ\text{C})$$

$$\log(D_{chem}[\text{CM}^2 \text{ c}^{-1}]) = -7.2 \pm 0.5 (500 \text{ } ^\circ\text{C})$$

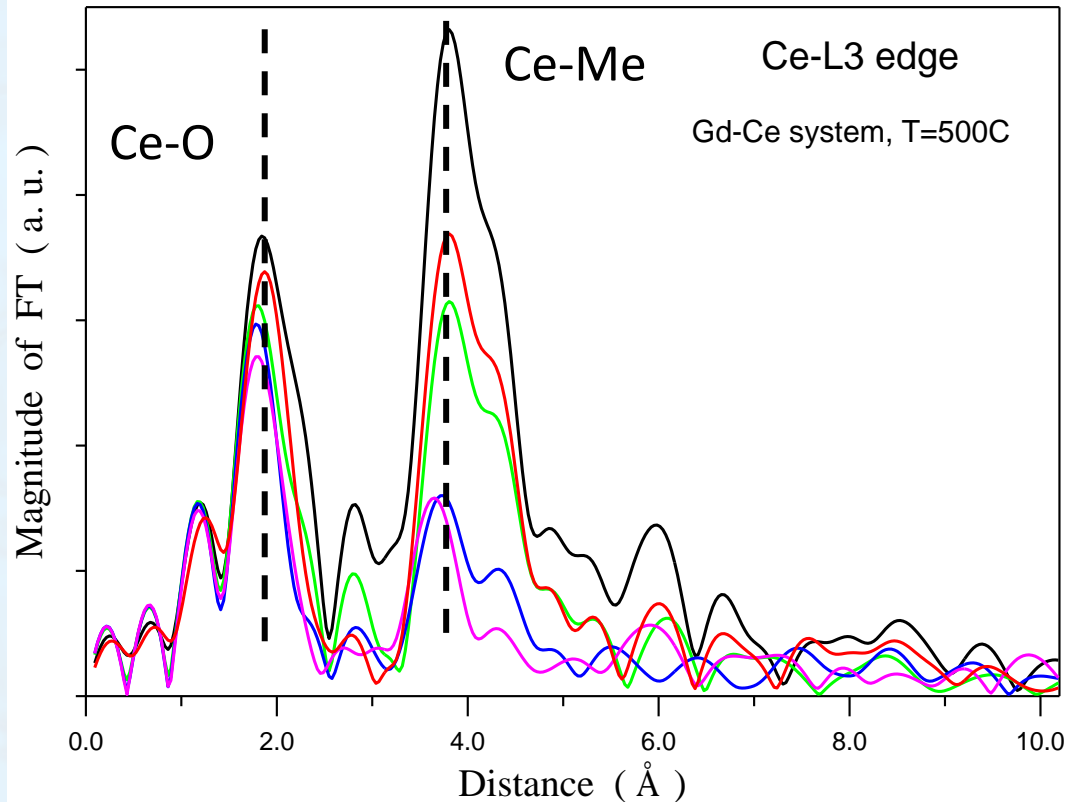
D_O scale



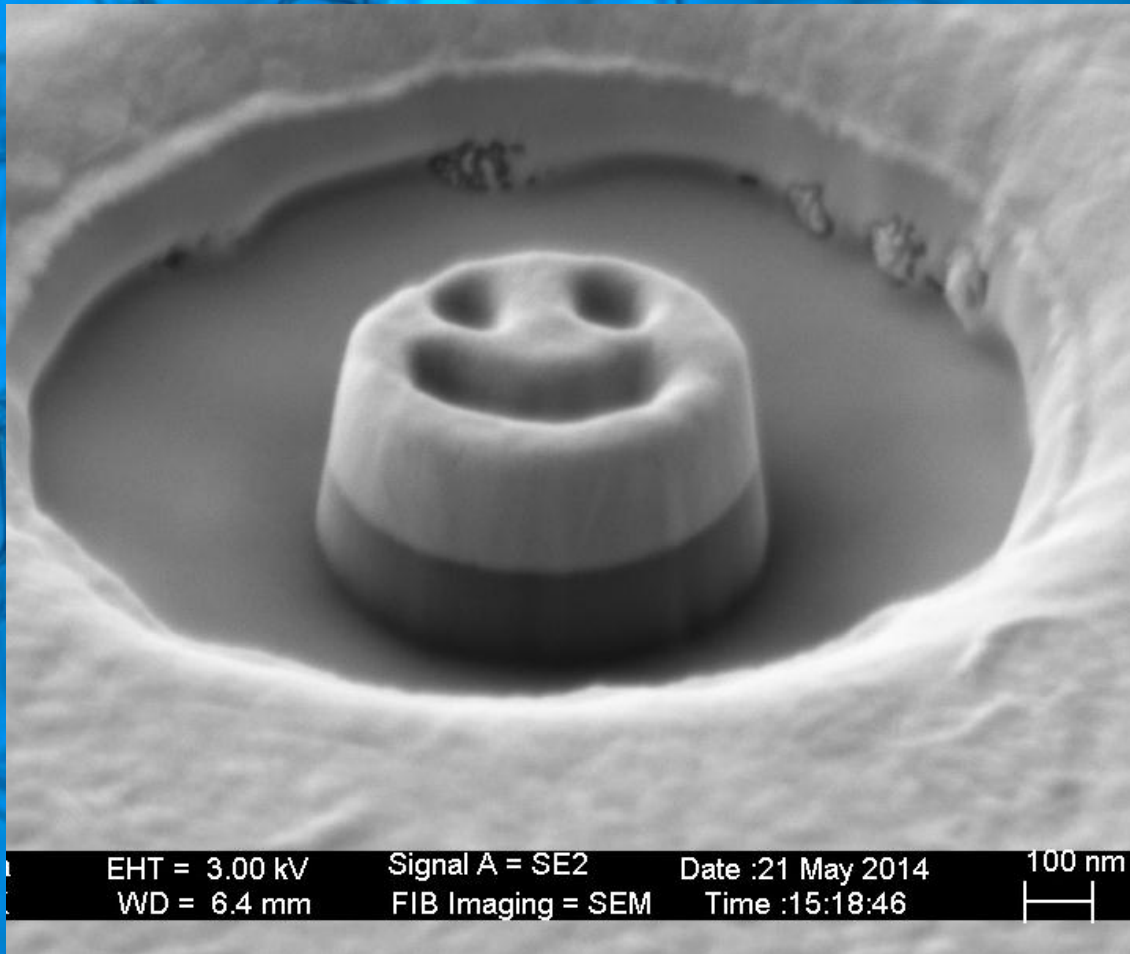
Ni_{0.5} – the most efficient, more pronounced effect of Ni content on fast channel via defects (up to 10% of total content in the bulk)

Pr deficiency in perovskite decreases migration barrier, but its content is still ~5%. Pr incorporation in fluorite decreases migration barrier due to a vacancies in Pr coordination sphere as proposed.

EXAFS

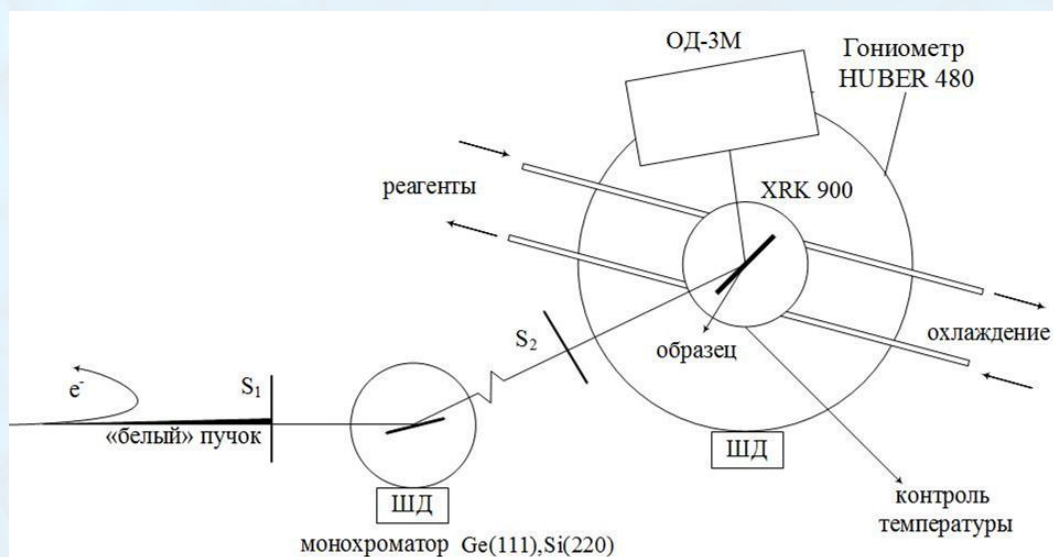
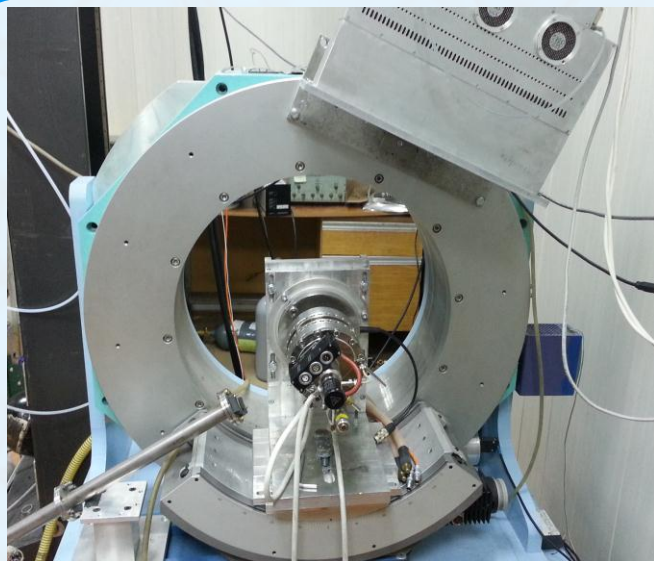


The intensity of the EXAFS peaks corresponding to the Ce-O and Ce-Me coordination shell declines with increasing dopant content. Lower Ce-O peak - higher $[V_O]$ in Ce vicinity.



Thank you for attention

Station at the 6th beamline



Общий вид и схема станции на канале №6 вывода СИ накопителя электронов ВЭПП-3.



Керамический держатель образца (слева).

SRS UGA-100 масс-спектрометр для контроля парциального давления кислорода. (справа)

